Lorente Crespo, M.; Wang, L.; Ortuño Molinero, R.; García Meca, C.; Ekinci, Y.; Martínez Abietar, AJ. (2013). Magnetic hot spots in closely spaced thick gold nanorings. Nano Letters. 13(6):2654-2661. doi:10.1021/nl400798s.

Magnetic hot spots in closely-spaced thick gold nanorings

María Lorente-Crespo,[†,¶] Li Wang,[‡,¶] Rubén Ortuño,[†] Carlos García-Meca,[†] Yasin Ekinci,[‡] and Alejandro Martínez[*,†]

Nanophotonics Technology Center, Universitat Politècnica de València, Camino de Vera, s/n, 46022, Valencia, Spain, and Laboratory for Micro- and Nanotechnology, Paul Scherrer Institute, 5232 Villigen PSI, Switzerland

E-mail: amartinez@ntc.upv.es

KEYWORDS: Surface plasmons, plasmonic array, nanoring, optical magnetism, magnetic enhancement, nanoantenna

Abstract

Light-interaction at optical frequencies is mostly mediated by the electric component of the electromagnetic field, being the response to the magnetic component usually negligible. Recently, it has be shown that properly engineered metallic nanoparticles can provide a magnetic response at optical frequencies originated from real or virtual flows of electric current in the structure. In this work, we demonstrate a new plasmonic mode which emerges from the strong coupling of high-aspect ratio gold nanorings. The resonance changes its character from electric to magnetic when increasing the height of the nanorings, giving rise to magnetic plasmons. Numerical simulations show that a virtual current loop appears at resonance for

[*]To whom correspondence should be addressed
[†]Nanophotonics Technology Center
[‡]Paul Scherrer Institute
[¶]Contributed equally to this work

sufficiently thick nanorings, causing a strong concentration of the magnetic field in the gap region (magnetic hot spot). We find that there is an optimum thickness that provides the maximum magnetic intensity enhancement (over 100-fold enhancement) and give an explanation of this observation. This strong magnetic dipolar resonance, observed both experimentally and theoretically, can be used in designing new metamaterials at optical frequencies.

Interaction between radiation and matter at optical frequencies is mostly mediated by polarization of atoms and molecules induced by the electric component of an incoming electromagnetic wave. Electric polarizability is the physical phenomenon behind the refractive index property of dielectric materials. Localized surface plasmon resonances (LSPRs) taking place when properly illuminating with near infrared (NIR) or visible light a nanoparticle made of a noble metal also arise as a consequence of the interaction of matter with the electric field. Such resonances, whose wavelength largely depends on the nanostructure shape and size, and the local dielectric environment, are typically caused by the accumulation of charges (conduction electrons) of opposite signs in different regions of the illuminated metal nanoparticle, which produces an effective electric polarization.[1] A key property of LSPRs is the possibility to concentrate light in subwavelength regions with electric field intensities enhanced up to several orders of magnitude, which has been sometimes referred to as electric hot-spots.[2] This property has been used to build plasmonic nanoantennas, which are metallic nanostructures designed to localize and concentrate strongly the electric field in a subwavelength region,[3] as well as to develop ultrasensitive sensors.[4]

On the contrary, magnetic activity at optical frequencies is about four order of magnitude smaller than its electric counterpart because matter response to the magnetic component of light is extremely weak. In fact, it is widely accepted that there is no any natural medium magnetically active at optical frequencies.[5] However, we could think that nanostructuring metals is a way to strengthen the magnetic response at optical frequencies, as it occurs for the electric field. In fact, it has been shown that LSPRs can have a magnetic character, which gives rise to magnetic activity in the optical regime.[6,7] In this case, the underlying atoms or molecules are not magnetically polarized. Instead, it is the generation of surface currents on metallic surfaces as a consequence of

external illumination what produces a magnetic moment that interacts with the incident field. A typical requirement to get magnetic activity at optical frequencies is to have two parallel metallic plates in close proximity so that the incoming magnetic field parallel to the plates can create a virtual current loop (VCL) that gives rise to another magnetic field which sums up to the incoming one.[8,9] This kind of LSPR is commonly referred to as magnetic plasmon[7] and is the ultimate responsible for the magnetic response in fishnet metamaterials.[10] Other configurations to get magnetic plasmons have also been proposed, such as by self-assembled nanoparticle clusters,[11] both approaches sharing the creation of a VCL under proper illumination as the mechanism that produces the magnetic response. Interestingly, the created VCL between adjacent metallic plates can also give rise to a strong confinement of the local magnetic field in the subwavelength gap (magnetic hot-spot).[12] Lately it has also been predicted that this strong concentration of the magnetic field also appears in some nanoantennas, such as the diabolo antenna[13] and the complementary bowtie antenna.[14] It should be noticed that in such nanoantennae the local magnetic enhancement do not arise from a VCL between parallel plates but as a consequence of real current flowing through a thin metallic wire. Therefore, metallic nanostructures do not only provide a powerful way to concentrate the electric field, but also to locally enhance the magnetic field, which could find new unprecedented applications.

In this work, we show both numerically and experimentally that a strong magnetic response in the NIR is attained by illuminating subwavelength-spaced thick gold nanorings. If the nanorings are thin, the LSPR displays a pure electric behavior which gives rise to a strong enhancement of the electric field in the gap (coupled-bonding mode).[15] However, when the height of the nanorings is increased so that it is much larger than the spacing between them, a VCL appears between the nanorings which provides a strong magnetic field concentration in the gap, giving rise to a magnetic hot-spot. In fact, our results show that the LSPR changes from a electric to a magnetic character for sufficiently thick nanorings and find than there is an optimum thickness that maximizes the magnetic field enhancement in about two orders of magnitude. The VCL also originates a magnetic dipole that can result in strong magnetic activity in the far field. We observe experimentally the

resonance in arrays of coupled gold nanorings and its red-shifting when the nanoring thickness is increased as expected from numerical simulations. Two coupled thick nanorings could be used as an optical nanoantenna if isolated (we will argue that its behavior would be identical to that of a magnetic nanoloop) or for building optical materials with enhanced magnetic activity when arranged in an array.

An isolated gold nanoring supports two main LSPRs that can be explained from the hybridization of the resonances of a disk and a hole.[16] These two resonances are usually called bonding (or symmetric) and antibonding (or antisymmetric) modes, taking place in the NIR and visible wavelength regions respectively. The bonding mode displays charge concentrations of different signs at the opposite sides of the nanoring, which results in a considerable electric dipole that gives rise to intense local electric fields.[17] This also means that this LSPR has an electric character which should be manifested in producing a far field similar to that of an electric dipole at the resonance wavelength. When two nanorings are put together, the resulting dimer also displays a bonding resonance (which is called coupled-bonding resonance) that inherits the main properties of the resonance of an isolated nanorings except for very small gap distances where higher-order modes arise as a consequence of the splitting of the bonding mode.[15] Interestingly, such nanoring dimers can display a huge concentration of the electric field in the subwavelength gap region,[15] which can become much higher than what is observed for an isolated nanoparticle.[17]

If the gold nanorings are arranged in a periodic lattice, the response will become completely polarization independent at normal incidence even for very small gaps. Moreover, the structure will be more dense which will facilitate the characterization in the laboratory by means of straightforward techniques. If the period of the array p is smaller than the resonance wavelength divided by the index of the underlying substrate n, diffraction effects are avoided[18] and the array response in the NIR region should be dominated by the excitation of coupled-bonding mode regardless of the polarization. This is confirmed by numerical simulations performed using the commercial software CST Microwave Studio, a three-dimensional electromagnetic simulator based on the finite integration technique. We consider a square array of gold nanorings with outer radius R_{out},

inner radius R_{in} and thickness t on top of a quartz substrate (see Fig. 1(a)). The spacing between neighbor nanorings is $s = p - 2R_{out}$. The gold is modeled by using values of the permittivity obtained experimentally by ellipsometry (see Supporting Information) whereas the quartz is modeled as a dielectric with index $n = 1.544$. The extinction spectrum of an array of gold nanorings with $t = 50$ nm, $R_{out} = 250$ nm, $R_{in} = 150$ nm and $s = 60$ nm plotted in Fig. 1(b) displays a great resemblance with the results presented in Ref.[15] for an isolated dimer. Therefore, we can state that the observed extinction peak correspond to the excitation of the coupled-bonded mode of nanoring dimers extended over the whole lattice. The observed shoulder at 865 nm corresponds to the Wood's anomaly for the substrate, in good agreement with the theoretical prediction. Since we are exciting the coupled-bonding mode, we can expect a strong concentration of the electric field in the gap between adjacent nanorings for sufficiently small s values when illuminated by NIR radiation at normal incidence. This is confirmed by our simulations as shown in Fig. 1(c) representing the electric field enhancement as $I_E = |E|^2/|E_0|^2$, where the electric field is measured at a point equidistant from the nanorings and at a height $t/2$ over the substrates with (E) and without (E_0) nanorings. As in the case of the dimers, for very small gap distances the bonding resonance will split up, although in the case of the array the situation is even more complex since each nanoring is coupled to four neighbors. The study of this splitting is out of the scope of this work and will be considered elsewhere.

In all previous studies of the optical response of gold nanorings (isolated, or forming dimers and arrays) relatively thin metal layers have been considered.[19] It would be interesting to know what happens when the metal thickness is increased. If the metal is thick enough, the region between nanorings closely resembles a pair of coupled nanoplates, which has been shown to support a magnetic plasmon resonance[7,8] and an enhancement of the magnetic field in the gap region[20] as a consequence of the formation of a VCL. The VCL is formed by opposite currents flowing along the nanorings surfaces and displacement currents flowing across the gap which close the loop.[7] As in the case of the electric field, we can study the magnetic field enhancement in the gap by means of the parameter $I_M = |H|^2/|H_0|^2$ being the magnetic field monitored at the same point as before.

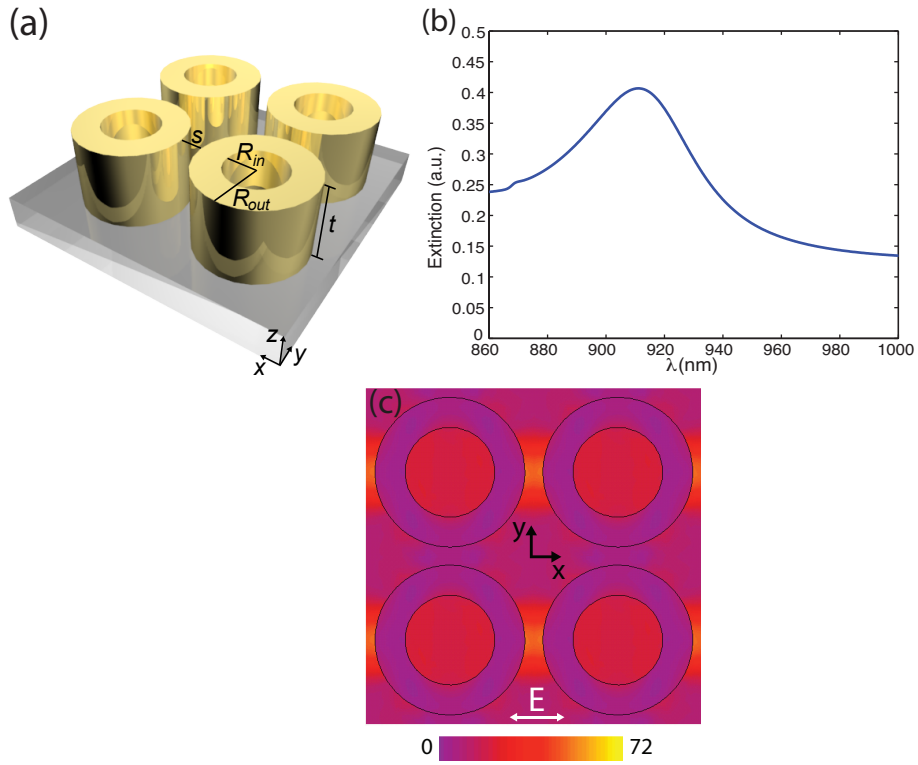

Scheme 1: (a) Array of gold nanorings with inner radius R_{in}, outer radius R_{out}, thickness t and separation between rings s. The nanorings are placed on top of a dielectric substrate with refractive index n; (b) Extinction coefficient of the array of gold nanorings with $t = 50$ nm, $R_{out} = 250$ nm, $R_{in} = 150$ nm and $s = 60$ nm. A quartz substrate is considered; (c) I_E measured at 910 nm for the same configuration as in (b).

Figure 2 plots the electric and magnetic fields enhancement as a function of the metal thickness for three different values of the nanoring spacing ($s = 10$ nm, $s = 30$ nm and 60 nm). It can be seen that for thin nanorings, the electric field is greatly enhanced, in agreement with previous observations,[15] but the magnetic field is comparable to the case with no nanorings (no enhancement). However, when $t > 150$ nm there is a growth of the I_M parameter which is accompanied by a reduction of the I_E parameter. This means that for sufficiently thick nanorings, we do not only observe a great enhancement of the magnetic field in the gap (a magnetic hot-spot), but a decrease of the electric field concentration. Indeed, for $t > 250$ nm we get that $I_M > I_E$. It can be said that the excited LSPR changes its character from electric to magnetic for sufficiently thick nanorings. In other words, for thin nanorings the LSPR resembles an electric dipole whilst for thick nanorings the LSPR mimics a magnetic dipole. This behavior has not been reported before to the best of our knowledge.

In addition, we notice that I_M reaches a maximum at $t = 270$ nm for both spacings under consideration ($I_M = 114$ for $s = 30$ nm and $I_M = 83$ for $s = 60$ nm) so there is an optimum metal thickness that maximizes the magnetic field enhancement. The explanation of the optimum thickness to maximize I_M is strongly related with the generation of VCLs as depicted in Fig. 3. For small values of t (Fig. 3(a)), the opposite currents generated at each side of the gap have small distance to travel and the induced magnetic field is small. Roughly speaking, it can be said that there is no space enough for the loop to be formed. For higher values of t (Fig. 3(b)), the electric current has distance enough to flow and an VCL is formed, causing the magnetic field concentration in the center of the loop. However, if t is too large (Fig. 3(c)), the metal-induced losses will be very high, which reduces the flow of current and, as a consequence, the induced magnetic field. Therefore, an array of coupled thick gold nanorings will produce an array of spots with high magnetic field concentration under normal illumination as depicted in Fig. 4. It has to be emphasized that an isolated nanoring would only interact with the local electric field. It is the combination of a small spacing gap together with tall metal walls which produce the observed magnetic resonance.

In all previous results we have considered the fields and the currents at resonance, this is, at the wavelength where the extinction reaches a maximum. Our calculations show that the resonant wavelength strongly depends on the metal thickness, as shown in Fig. 2(c). In fact, we have observed that for thin nanorings ($t < 150$ nm) for which the resonance has an electric behavior the resonance is kept approximately constant. However, as the thickness is increased so that the resonance enters the magnetic regime, we observe a strong red-shifting which can be considered as a clear signature of the magnetic-resonance. This red-shifting when the resonance turns from electric to magnetic has been observed before in other systems.[6] It has to be stressed that there are no significant diffraction effects in the wavelength region under consideration. For the arrays under consideration in Figs. 2-4 the Wood's anomaly falls at 1 μm for $s = 60$ nm and 960 nm for $s = 960$ nm, so we can assume that the observed extinction peak does not come from the periodicity but from local responses of the nanorings.

To fabricate the designed arrays, a thick polymer resist layer, *Poly*(methyl methacrylate) (PMMA),

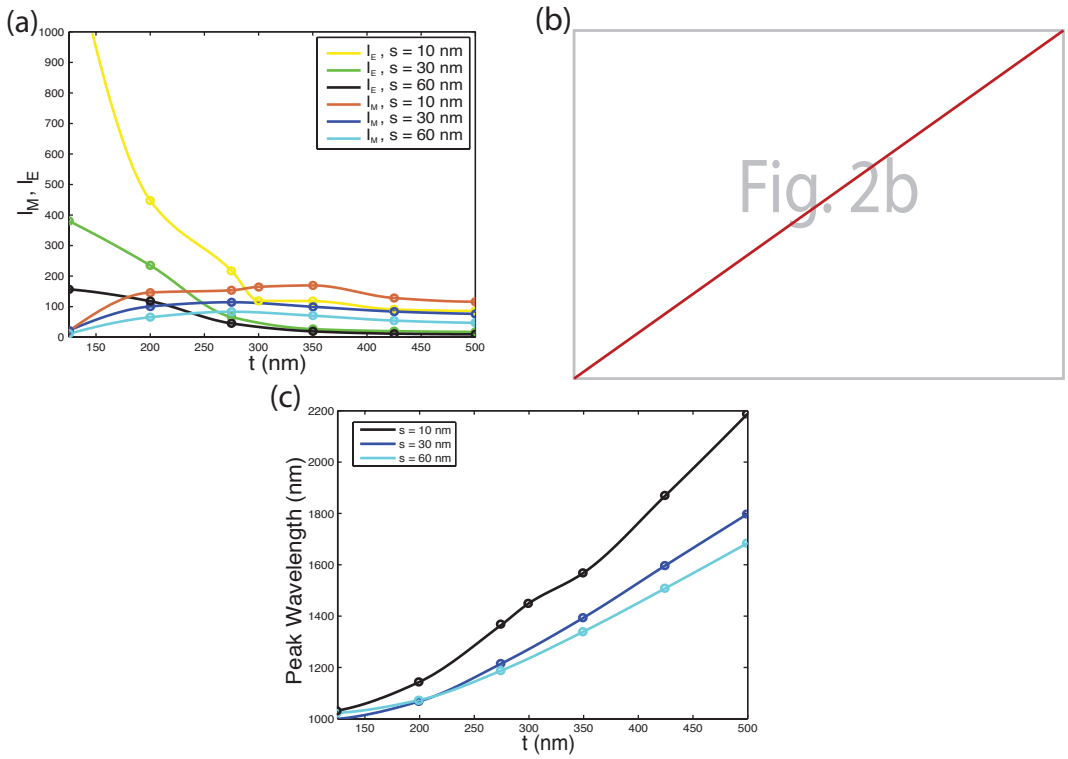

Scheme 2: (a) Calculated values of I_E and I_M as functions of the nanoring thickness for different nanorings spacings . The array is illuminated normally at a wavelength at which the extinction reaches a maximum. (b) I_E and I_M as functions of the spacing for a fixed thickness $t = 275$ nm. (c) Resonant wavelength as a function of the metal thickness for two different separation distances between nanorings (10, 30, 60 nm).

was deposited onto an electroplating base coated quartz substrate, which was then patterned using a Vistec EBPG5000Plus electron-beam lithography tool operated at 100 keV electron energy. The high energy enables electrons to penetrate deep into resists with little scattering. After development, the resist voids were filled with gold by electroplating, and the remaining PMMA mold was subsequently removed by oxygen plasma etching. The powerful electron beam tool provided precise structuring at the nanoscale,[21] which allowed us to fabricate a wide range of nanoring structures of varying diameter, spacing and height, resulting in various aspect-ratios. In contrast to fabrication based on lift-off,[19] thicker nanorings can be attained by this technique. More details about the fabrication of the samples can be found in the Supporting Information. Some images of the fabricated samples obtained by scanning electron microscopy (SEM) are shown in Fig. 5.

Experimental extinction spectra of the fabricated samples were collected by means of a Bruker

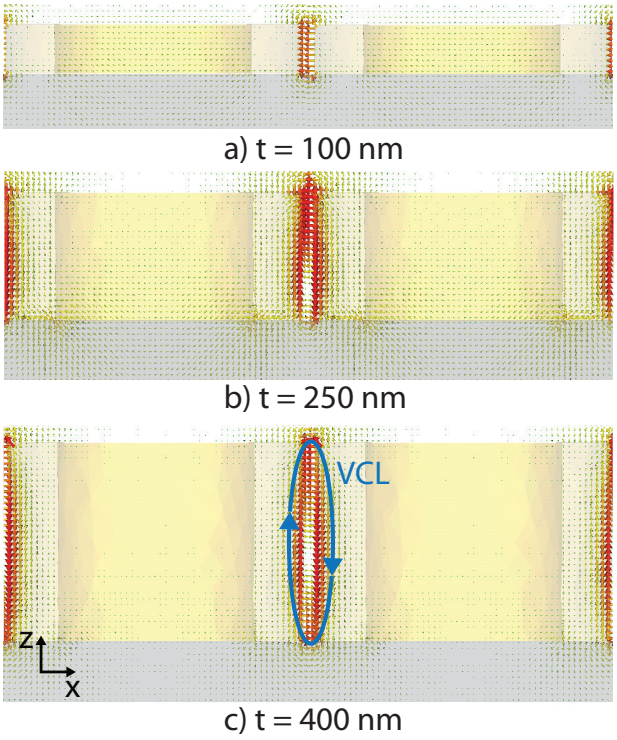

Scheme 3: Currents generated in a pair of coupled nanorings for different values of the metal thickness. An VCL (depicted in (c)for clarity) is formed in the gap under normal illumination, being responsible for the enhancement of the magnetic field.

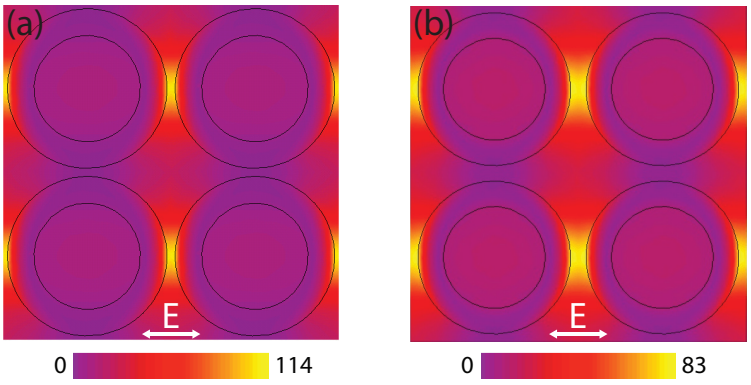

Scheme 4: Map of I_M when the array is illuminated at normal incidence at the resonance wavelength when the separation between adjacent rings is (a) $s = 30$ nm, and (b) $s = 60$ nm. For unpolarized light the magnetic hot-spots will appear in all the gaps

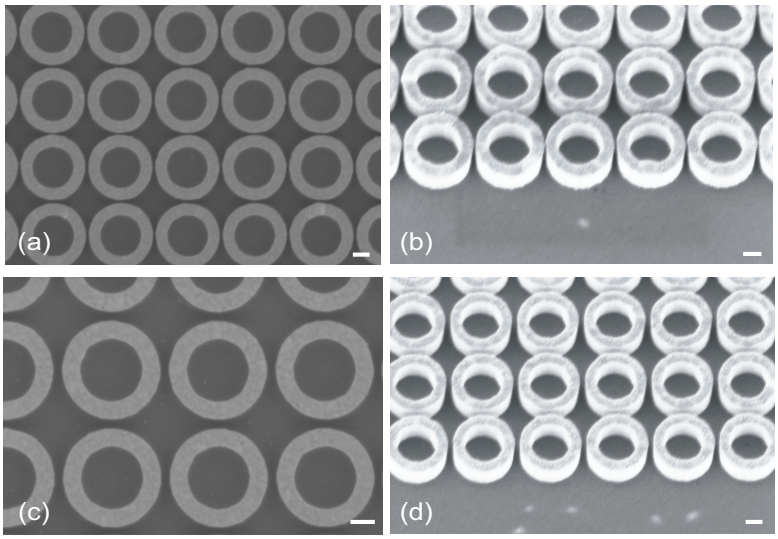

Scheme 5: Scanning electron microscope images of fabricated samples with $t = 350$ nm, $R_{out} = 300$ nm and $R_{in} = 200$ nm. Measured values of these parameters were within ± 5 nm of the nominal values. (a), (c) $s = 30$ nm, (b), (d) $s = 60$ nm. Image (a) and (b) are taken from the top and (c) and (d) at a 25° tilt angle. Scale bars are all 200 nm.

Vertex 80 Fourier-transform interferometer (FTIR) spectroscopy system. The obtained results for different values of the nanoring thickness are shown in Fig. 6. Simulation results are overimposed. The red-shift of the resonance frequency when t grows is clearly observed, which is a clear signature of the transition from the electric to magnetic character, as previously mentioned. It can be observed that simulations are in good agreement with measurements. The larger experimental peak widths are probably due to an inhomogeneous broadening since multiple nanorings are simultaneously illuminated and their dimensions can differ slightly.

The resonance wavelength of the magnetic LSPR depends on several parameters that permits us to tune the response over the whole NIR range. For instance, the resonance wavelength depends strongly on the refractive index of the underlying substrate, as noticed in previous works. Figure 7(a) shows the extinction spectra for quartz and glass ($n = 1.45$) substrates. It can be seen that the response is blue-shifted for the glass substrate as a consequence of its smaller index of refraction. A fine tuning can be achieved by properly adjusting the inner radius R_{in}, as shown in Fig. 7(b).[17,22] It can be seen that the response is slightly blue-shifted when R_{in} decreases, in agreement with the behavior of the electric LSPR of thin gold nanorings.[17] It has to be mentioned that when $R_{in} = 0$ we

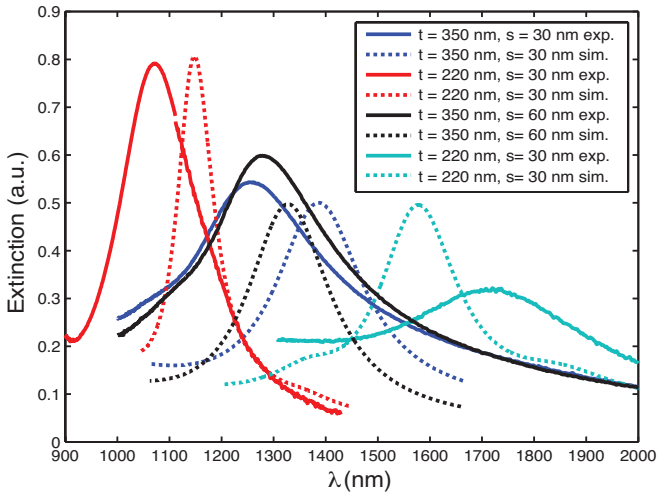

Scheme 6: Measured and simulated extinction spectra of arrays of gold nanorings on quartz with $R_{out} = 300$ nm and $R_{in} = 200$ nm for different values of t and s.

get an array of coupled gold nanodisks. In this case, the main properties of the observed magnetic plasmon, such as the high magnetic field concentration, are conserved. Therefore, a coupled-disk array would also be a proper platform to observe the effects arising from the excitation of the magnetic plasmon.

The array of thick nanorings converts the incoming light into localized magnetic field spots with an intensity enhancement over 100. In other words: our structure works as an array of magnetic nanoantennas. The arrangement in an array will provides a very dense periodic structure of magnetic hot spots (about 500 millions per cm^2 in the fabricated samples) when illuminating the nanorings with unpolarized light at the resonant wavelength. Each nanoantenna will be formed by two closely-spaced nanorings whose performance mimics an electrically-large resonant nanoloop. Indeed, a loop antenna is at resonance at a wavelength equal to its perimeter. In our case, the resonance (see Fig. 2(c)) occurs at wavelength about 1.5-2 times the perimeter (obtained as $2s+2t$). However, this can be explained by the penetration of the fields inside both the metal and the dielectric substrate, which is well-know to produce an increase in the wavelength of the LSPR, as in the case of dipole nanoantennas.[3] Therefore, it is reasonable to think that our structure performs as an array of resonant nanoloops. Future work will address the far-field radiation properties of the

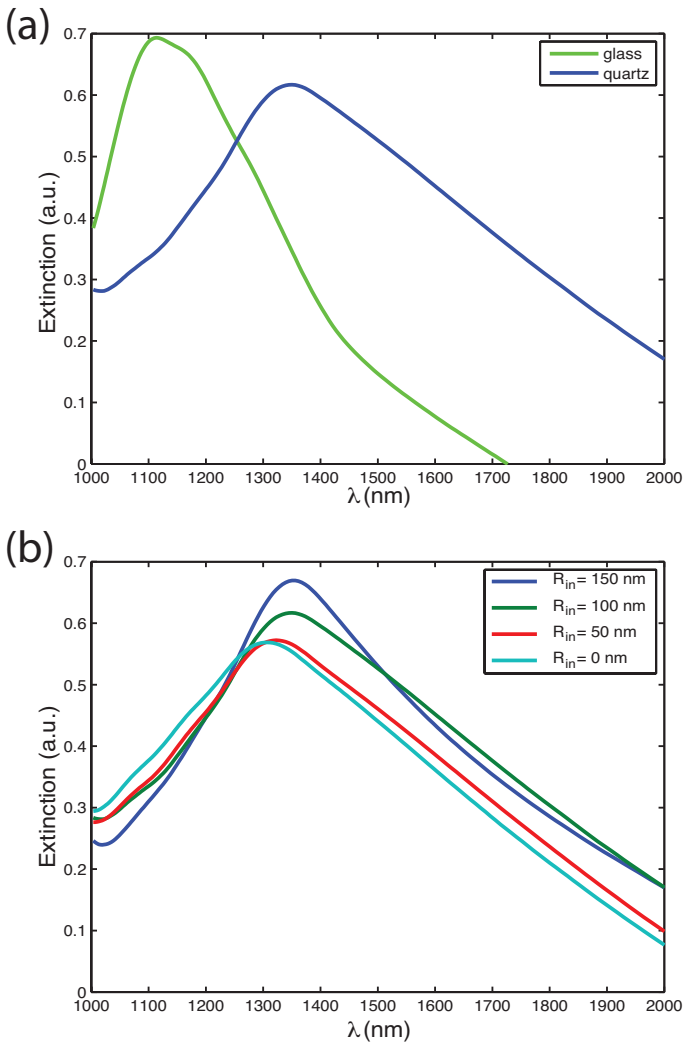

Scheme 7: Measured extinction spectra of different nanoring arrays with $t = 175$ nm, $R_{out} = 325$ nm and $s = 120$ nm. (a) Different responses for quartz and glass substrates ($R_{in} = 120$ nm). (b) Different response as a function of the inner radius R_{in} (quartz substrate).

nanoring arrays.

The magnetic field enhancement observed in the fabricated structures at NIR wavelengths (around 1500 nm) is of the same order of magnitude than in diabolo[13] or complementary bowtie[23] nanoantennas in which the magnetic enhancement is achieved through high real current flow along very thin metallic wires. The enhancement can be even improved by selecting a material with more appropriate properties, such as a higher value of the imaginary part of the index of refraction.[24] For instance, if we employe a Drude model for the gold nanorings, we get enhancement values

above 200 at wavelengths in the NIR (see Supporting information). This also means that it would be easier to achieve very-strong enhancements at longer wavelengths where the imaginary part of the refractive index is higher for most metals. In comparison with horizontal parallel nanoplates which also permit the excitation of magnetic plasmon as well as the concentration of the magnetic field, in our case we do not need the existence of a dielectric spacing a layer between metallic walls. This means that the region of magnetic field localization is accessible from the outside so it could be used for applications such as sensing, manipulation or trapping.

In summary, we have shown that the LSPR of coupled gold nanorings turns from an electric to a magnetic character (magnetic plasmons) for sufficiently thick nanorings. A high magnetic field concentration (magnetic hot-spot) with enhancement values over 100 takes place in the sub-wavelength gap region for normal illumination. As a result, an array of such nanorings acts as an array of magnetic nanoantennae mimicking resonant nanoloops in which the incoming propagating light in converted into a strongly localized magnetic field. The induced VCLs will therefore create strong magnetic dipoles which could be used to build magnetically-active metamaterials in the optical domain.

Supporting Information Available

^{1}H NMR, FTIR, and WAXS characterization of random copolymers and a comparison of the two methods for measuring τ_b^* are given in the Supporting Information. This material is available free of charge via the Internet at `http://pubs.acs.org/`.

Acknowledgement

This work has been supported by Spanish Government and European Union (EU) funds under contracts CSD2008-00066 and TEC2011-28664-C02-02, and Universitat Politecnica de Valencia (program INNOVA 2011).

References

(1) Barnes, W. L.; Dereux, A.; Ebbesen, T. W. T. *Nature* **2003**, *424*, 824–830.

(2) Schuller, J.; Barnard, E.; Cai, W.; Jun, Y.; White, J.; Brongersma, M. *Nature materials* **2010**, *9*, 193–204.

(3) Mühlschlegel, P.; Eisler, H.; Martin, O.; Hecht, B.; Pohl, D. *Science* **2005**, *308*, 1607.

(4) Larsson, E. M.; Alegret, J.; Käll, M.; Sutherland, D. S. *Nano letters* **2007**, *7*, 1256–1263.

(5) Landau, L. D.; Lifshitz, E. M.; Pitaevskii, L. P. In *Course of Theoretical Physics*; Landau, L. D., Lifshits, E. M., Eds.; Landau and Lifshitz Course of Theoretical Physics 14; Pergamon Press, 1984; Vol. 8; p 460.

(6) Alù, A.; Engheta, N. *Optics express* **2009**, *17*, 5723–5730.

(7) Sarychev, A.; Shvets, G.; Shalaev, V. *Physical Review E* **2006**, *73*, 1–10.

(8) Ortuño, R.; García-Meca, C.; Rodríguez-Fortuño, F.; Martí, J.; Martínez, A. *Physical Review B* **2009**, *79*, 75425.

(9) Huang, Z.; Xue, J.; Hou, Y.; Chu, J.; Zhang, D. *Physical Review B* **2006**, *74*, 1–4.

(10) García-Meca, C.; Hurtado, J.; Martí, J.; Martínez, A.; Dickson, W.; Zayats, A. *Physical Review Letters* **2011**, *106*, 67402.

(11) Fan, J.; Wu, C.; Bao, K.; Bao, J.; Bardhan, R.; Halas, N.; Manoharan, V.; Nordlander, P.; Shvets, G.; Capasso, F. *science* **2010**, *328*, 1135.

(12) Pakizeh, T.; Abrishamian, M.; Granpayeh, N. *Optics Express* **2006**, *14*, 8240–8246.

(13) Grosjean, T.; Mivelle, M.; Baida, F. I.; Burr, G. W.; Fischer, U. C. *Nano letters* **2011**, 1009–1013.

(14) Zhou, N.; Kinzel, E. C.; Xu, X. *Optics letters* **2011**, *36*, 2764–2766.

(15) Tsai, C.-Y.; Lin, J.-W.; Wu, C.-Y.; Lin, P.-T.; Lu, T.-W.; Lee, P.-T. *Nano Letters* **2012**, *12*, 1648–1654.

(16) Ye, J.; Van Dorpe, P.; Lagae, L.; Maes, G.; Borghs, G. *Nanotechnology* **2009**, *20*, 465203.

(17) Aizpurua, J.; Hanarp, P.; Sutherland, D.; Käll, M.; Bryant, G.; García de Abajo, F. *Physical Review Letters* **2003**, *90*, 5–8.

(18) Ebbesen, T. W.; Lezec, H. J.; Ghaemi, H. F.; Thio, T.; Wolff, P. A. *Nature* **1998**, *391*, 667–669.

(19) Near, R.; Tabor, C.; Duan, J.; Pachter, R.; El-Sayed, M. *Nano letters* **2012**, *12*, 2158–64.

(20) Tang, C. J.; Zhan, P.; Cao, Z. S.; Pan, J.; Chen, Z.; Wang, Z. L. *Physical Review B* **2011**, *83*, 41402.

(21) Päivänranta, B.; Merbold, H.; Giannini, R.; Büchi, L.; Gorelick, S.; David, C.; Löffler, J.; Feurer, T.; Ekinci, Y. *ACS Nano* **2011**, *5*, 6374–6382.

(22) Prodan, E.; Radloff, C.; Halas, N. J.; Nordlander, P. *Science (New York, N.Y.)* **2003**, *302*, 419–22.

(23) Zhou, L.; Wang, Q.-j.; Wu, S.; Huang, W.; Huang, C.-p.; Zhu, Y.-y. *JOSA B* **2011**, *28*, 587–591.

(24) Merlin, R. *Proceedings of the National Academy of Sciences of the United States of America* **2009**, *106*, 1693–8.